

Slip Flow Convection Heat Transfer in a Rectangular Microchannel with Exponential Wall Heat Flux

H. Shokouhmand, S. Jomeh

Abstract— Slip-flow convection heat transfer in thermal entry region of a rectangular microchannel is investigated. The wall heat flux is peripherally constant and varies exponentially with respect to the axis of the microchannel. The flow is assumed to be hydrodynamically fully developed. The three-dimensional energy conservation equation is solved numerically for different aspect ratios. Surface interaction parameters consist of momentum accommodation coefficient and thermal accommodation coefficient, are introduced to the simulation and their effects on heat transfer is investigated. The fully-developed Nusselt numbers are obtained for different values of the parameter defined in the exponential function of heat flux. For a special case, i.e., constant wall heat flux, the results are compared with those presented in literature. It was observed that two dimensionless variables that include rarefaction and surface interactions affect Nusselt number. For a specific value of thermal dimensionless variable, there is a transition region between continuum regime and slip-flow regime. Beyond this value, Nusselt number decreases as the momentum dimensionless variable increases.

Index Terms—Microchannel, Numerical analysis, Nusselt number, Slip-flow convection

I. INTRODUCTION

As the size of the electronic devices reduces, the need for cooling equipments that dissipate maximum amount of heat per unit area increases. Along the development of micro-electro-mechanical systems (MEMS), microscale heat transfer has gained great interests in recent years. Among these, microchannels are of particular importance due to their high rates of heat dissipation and small size.

As the size of a microchannel decreases, the continuum assumption of the flow is no longer valid and some deviations are observed when compared with macroscale flow. It is

demonstrated that rarefaction effects include velocity slip and temperature jump at the walls, must be considered. These effects occur in microscale flows or at low-pressure gas flows. For measuring of the degree of rarefaction, the Knudsen number is defined. Knudsen number is the ratio of the mean free path to the macroscopic length scale of the flow and is used for classifying the flow regimes. There is a specific range for Kn that one can still apply Navier-Stokes equations with appropriate modifications on the boundary conditions [2], [8]. The flow in this range is called slip flow. Beskok *et al.* [1] give the range $0.001 < Kn < 0.1$ for the Knudsen number in the slip-flow regime. Most microscale thermal systems have characteristic length of the order 1-100 μm and the molecular mean free path of the order 100 nm. So the Knudsen number lies in the above range in most cases.

Sparrow *et al.* [4] and Inman [14] were the first who analyzed laminar slip-flow heat transfer for tubes with uniform heat flux and a parallel plate channel or a circular tube with uniform wall temperature. They pointed out that slip characteristics of the flow decrease the Nusselt number. Rosenow *et al.* [18] suggested that the entrance condition should be assumed as being hydrodynamically fully developed and thermally developing. Ameer *et al.* [17] and Baron *et al.* [11], [12] studied the Graetz problem for slip flow with constant-heat flux or constant-wall-temperature boundary conditions. Their results showed that velocity slip tends to increase heat transfer while temperature jump has the opposite effect. Tunc and Bayazitoglu [6] investigated analytically slip-flow regime for both hydrodynamically and thermally fully-developed inlet conditions, but they do not consider the temperature jump effect in their solution. Yu and Ameer [15], [16] studied analytically the heat transfer for thermal entry region of a microchannel with constant-wall-temperature and isoflux boundary conditions. Further studies have been performed by several researchers; e.g., Kavehpour *et al.* [7], Larrode *et al.* [5], Hadjiconstantino and Simek [9], Asako [19].

In all these studies the boundary conditions are to be met, include constant wall temperature or constant heat flux. No attempt has been observed for treating the case of exponential-varying wall heat flux boundary condition. In the present study, slip-flow heat transfer for thermal entry region of a microchannel is investigated under exponential heat flux boundary condition. The three-dimensional energy

Manuscript received March 11, 2007.

H. Shokouhmand is with the School of Mechanical Engineering, University of Tehran, P.O. Box 11365/4562, Tehran, Iran (corresponding author to provide phone: +98(21)-88005677; fax: +98(21)-88013029; e-mail: hshokoh@ut.ac.ir).

S. Jomeh is with the School of Mechanical Engineering, University of Tehran, P.O. Box 11365/4562, Tehran, Iran. (e-mail: sjomeh@ut.ac.ir).

conservation equation is solved numerically using a finite difference method for different aspect ratios. Rarefaction effects are also included. Results for the case of isoflux wall are in good agreement with those presented by Yu and Ameen [15]. The temperature distribution and fully developed Nusselt number are also obtained for different values of the parameters introduced to the problem.

II. ANALYSIS

The geometry of the problem is shown in Fig. 1. The center of the coordinate system is located at the bottom left corner of the channel. The dimensions of the channel in y and z directions are a and b respectively and x coordinate is measured along the axis.

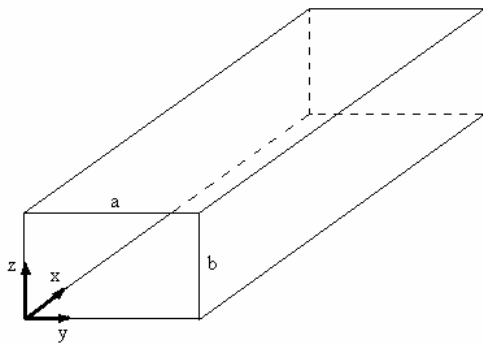


Fig. 1. The schematic of the microchannel

A. Streamwise Velocity Distribution

For steady state, incompressible flow with constant fluid properties, momentum conservation equation in fully-developed region can be written as follows

$$\frac{\partial^2 u}{\partial y^2} + \frac{\partial^2 u}{\partial z^2} = \frac{1}{\mu} \frac{dP}{dx}, \quad (1)$$

where u is the streamwise velocity, P is the pressure and μ is the dynamic viscosity. For slip-flow regime, the hydrodynamic boundary conditions are

$$u = u_s \quad \text{at } y=0, a \text{ and } z=0, b, \quad (2)$$

where u_s is the slip velocity at the walls. For example at $y=0$, u_s is [3], [10]

$$u_s = \beta_v \lambda \left. \frac{\partial u}{\partial y} \right|_{y=0}, \quad (3)$$

where λ is the molecular mean free path and

$$\beta_v = \frac{2 - F_v}{F_v}. \quad (4)$$

F_v , the tangential momentum accommodation coefficient, is a measure of degree of specular reflection and diffuse reflection for the fluid molecules that collide with the wall. This coefficient depends on several parameters such as surface roughness, but it is near unity for most engineering applications [3].

For nondimensionalizing the equations above, following variables are defined

$$u^* = \frac{u}{u_m}, \quad y^* = \frac{y}{a}, \quad z^* = \frac{z}{a}, \quad (5)$$

where u_m is the mean streamwise velocity. The governing equation and the boundary condition; e.g. at $y=0$, take the form below

$$P^* = \frac{\partial^2 u^*}{\partial y^{*2}} + \frac{\partial^2 u^*}{\partial z^{*2}}, \quad (6)$$

$$u^*_{(0,z^*)} = \beta_v Kn \left. \frac{\partial u^*}{\partial y^*} \right|_{y^*=0}, \quad (7)$$

where Kn is the Knudsen number and P^* is the dimensionless pressure wick defined as

$$P^* = \frac{a^2}{\mu u_m} \frac{\partial P}{\partial z}, \quad (8)$$

$$Kn = \frac{\lambda}{a}. \quad (9)$$

Tunc and Bayazitoglu [6] have solved (6) with its boundary conditions using the integral transform technique. Here, their results are used to solve the energy equation.

B. Temperature Distribution

The following assumptions have been made to solve the energy equation:

- steady state flow,
- constant fluid properties,
- negligible viscous dissipation ,
- negligible axial conduction within the domain and at the walls.

So, the energy equation takes the following form

$$\frac{u}{\alpha} \frac{\partial T}{\partial x} = \frac{\partial^2 T}{\partial y^2} + \frac{\partial^2 T}{\partial z^2}, \quad (10)$$

where T is the fluid temperature and α is the thermal diffusivity. Considering inwardly-imposed heat flux, the boundary conditions are

$$T_{(0,y,z)} = T_e, \quad (11)$$

$$k \frac{\partial T}{\partial y} = q'' \quad \text{at } y=0, \quad (12)$$

$$k \frac{\partial T}{\partial y} = q'' \quad \text{at } y=a, \quad (13)$$

$$k \frac{\partial T}{\partial z} = q'' \quad \text{at } z=0, \quad (14)$$

$$k \frac{\partial T}{\partial z} = q'' \quad \text{at } z=b, \quad (15)$$

where T_e is the entrance fluid temperature, k is the thermal conductivity, q'' is the wall heat flux and it can be written as follows

$$q'' = q''_0 \exp\left(\frac{mx^*}{2}\right). \quad (16)$$

m is an arbitrary parameter that can be varied and

$$x^* = \frac{x}{\frac{D}{2}Pe}, \quad (17)$$

where Pe is the Peclet number and D is the hydraulic diameter
 $Pe = RePr$, (18)

$$D = \frac{2ab}{a+b}. \quad (19)$$

Nondimensionalizing of (10)-(15) gives

$$u^* \frac{\alpha'^2}{2} \frac{\partial \theta}{\partial x^*} = \frac{\partial^2 \theta}{\partial y^{*2}} + \frac{\partial^2 \theta}{\partial z^{*2}}, \quad (20)$$

$$\theta_{(0,y^*,z^*)} = 0, \quad (21)$$

$$\left(\frac{\partial \theta}{\partial y^*} \right)_{y^*=0} = -\frac{\alpha'}{2} \exp\left(\frac{mx^*}{2}\right), \quad (22)$$

$$\left(\frac{\partial \theta}{\partial y^*} \right)_{y^*=1} = \frac{\alpha'}{2} \exp\left(\frac{mx^*}{2}\right), \quad (23)$$

$$\left(\frac{\partial \theta}{\partial z^*} \right)_{z^*=0} = -\frac{\alpha'}{2} \exp\left(\frac{mx^*}{2}\right), \quad (24)$$

$$\left(\frac{\partial \theta}{\partial z^*} \right)_{z^*=\gamma} = \frac{\alpha'}{2} \exp\left(\frac{mx^*}{2}\right), \quad (25)$$

where

$$\theta = \frac{T - T_e}{\frac{q_0'' D}{k}} \quad (26)$$

is the dimensionless temperature and

$$\alpha' = \frac{2a}{D} = \frac{1+\gamma}{\gamma}, \quad (27)$$

where

$$\gamma = \frac{b}{a}. \quad (28)$$

γ is the aspect ratio.

Equations (20)-(25) are solved numerically for different aspect ratios, rarefaction parameters and parameter m using finite-difference method. Temperature distribution is obtained for each case within the whole domain. An implicit method called ADI (Alternative Direction Implicit) is used in the present study. This method is implemented with some modifications in the nonslip case due to preventing the divergence that occurs on the boundaries. A computer program written in FORTRAN programming language is used here.

C. Nusselt Number

The Nusselt number is defined as below

$$Nu = \frac{\exp\left(\frac{mx^*}{2}\right)}{\theta_w - \theta_b}, \quad (29)$$

where θ_b and θ_w are the dimensionless bulk and wall temperatures respectively.

As mentioned earlier, velocity slip and temperature jump are two major effects of rarefaction. Velocity slip was introduced

to the momentum equation via hydrodynamic boundary condition. Temperature jump is used to describe the thermal boundary conditions at the walls. As it is presented in literature [3], temperature jump; e.g. at $y = 0$, can be given as

$$T_s - T_w = \left(-\beta_t \lambda \frac{\partial T}{\partial y} \right)_{y=0}, \quad (30)$$

where T_s is the temperature of fluid adjacent to the wall and

$$\beta_t = \frac{2 - F_t}{F_t} \frac{2R}{R+1} \frac{1}{Pr}, \quad (31)$$

where Pr is the Prandtl number and R is the specific heat ratio. F_t , the thermal accommodation coefficient, is a measure of ratio of specular and diffuse reflection again. This coefficient varies in a wide range from 0.01 to 1, but in most applications it is near unity [2]. Nondimensionalizing of (30) yields

$$\theta_w = \theta_s + \beta\beta_v Kn \frac{\alpha'}{2} \exp\left(\frac{mx^*}{2}\right) = \theta_s + \beta\beta' \exp\left(\frac{mx^*}{2}\right), \quad (32)$$

where β and β' are defined as below

$$\beta = \frac{\beta_t}{\beta_v}, \quad (33)$$

$$\beta' = \beta_v Kn \frac{\alpha'}{2}. \quad (34)$$

Substituting (32) into (29) gives

$$Nu = \frac{\exp\left(\frac{mx^*}{2}\right)}{\theta_s - \theta_b + \beta\beta' \exp\left(\frac{mx^*}{2}\right)}. \quad (35)$$

θ_b is defined as

$$\theta_b = \frac{1}{\gamma} \int_0^1 \int_0^1 u_{(y^*,z^*)} \theta_{(x^*,y^*,z^*)} dy^* dz^*. \quad (36)$$

Alternatively, bulk temperature can be obtained by applying the conservation of energy principle within a differential control volume and integrating the wall heat flux. After nondimensionalizing, the following relation can be derived

$$\theta_b = \begin{cases} \frac{4}{m} \left(\exp\left(\frac{mx^*}{2}\right) - 1 \right) & m \neq 0 \\ 2x^* & m = 0 \end{cases}. \quad (37)$$

Also, θ_s can be written as

$$\theta_s = \frac{\int_0^\gamma \theta_{(x^*,0,z^*)} dz^* + \int_0^\gamma \theta_{(x^*,1,z^*)} dz^* + \int_0^1 \theta_{(x^*,y^*,0)} dy^* + \int_0^1 \theta_{(x^*,y^*,\gamma)} dy^*}{2(1+\gamma)} \quad (38)$$

III. RESULTS AND DISCUSSION

As it may be seen from (16), for the case $m = 0$, the constant-heat flux boundary condition is met at the walls. So at first, this special case may be implemented for validating the solution. As the (34) and (35) show, the nonslip Nusselt numbers can be gained by setting $\beta_v Kn = 0$ or $\beta' = 0$. In Table I, these values for different aspect ratios are compared

with those presented in literature. Good agreement is achieved between the results especially for smaller aspect ratios.

As it is observed from the Table I, Nusselt number decreases with decreasing aspect ratio, but this variation is not considerable. This is in contrast with the results obtained with peripherally-constant-wall temperature constraint in where the Nusselt number augments drastically as the aspect ratio decreases. This is due to corner effects in the present study. The three-dimensional fully-developed temperature distributions for two aspect ratios; $\gamma = 1/4$ and $\gamma = 1$, and isoflux boundary conditions are shown in Fig. 2. It can be seen that the fluid temperature near the corners of the channel increases and this is more considerable in the lower aspect ratio case. So the average fluid temperature adjacent to the wall is greater than its value in the case of peripherally-constant wall temperature. This leads to augment the temperature difference between bulk and wall temperature and consequently decrease the Nusselt Number.

The three-dimensional temperature distribution for $\gamma = 1$ and $m = -1$ is plotted at two x^+ in Fig. 3. In contrast to the Fig. 2a, it is seen that the domain distribution tends to a constant temperature at large x^+ .

For better investigations, effects of variation of parameter m on the bulk temperature and the average surface temperature along the axis of the microchannel are shown in Fig. 4. As expected, for $m = 0$, i.e. isoflux condition, the variations of bulk and average surface temperature are linear with slope of 2 against x coordinate in fully-developed region. For $m = -1$, these two temperatures approach each other and to a constant value of $-4/m$ because of diminishing wall heat flux. This is the case that occurs for all negative values of m . The same behavior is observed for other aspect ratios and slip coefficients.

The fully-developed Nusselt numbers with respect to parameter m for various values of aspect ratio, β and β' are presented in Figs. 5, 6 and 7. As it is seen from these figures, Nusselt number shows different behaviors depending on the parameters defined in the problem. A greater value of β' results more momentum exchange between wall and fluid molecules, and consequently increases heat transfer. On the other hand, a greater value of β makes Nusselt number decrease according to (35). It is worth noting that parameter β

Table I. Comparison of nonslip fully-developed Nusselt number

γ	1	1/2	1/3	1/4	1/6	1/8
Present study	3.07	3.01	2.97	2.95	2.93	2.93
Iqbal <i>et al.</i> [13]	3.09	3.02	2.97	2.94	2.93	2.94
Yu and Ameer [15]	3.14	3.07	3.00	2.98	2.96	2.95

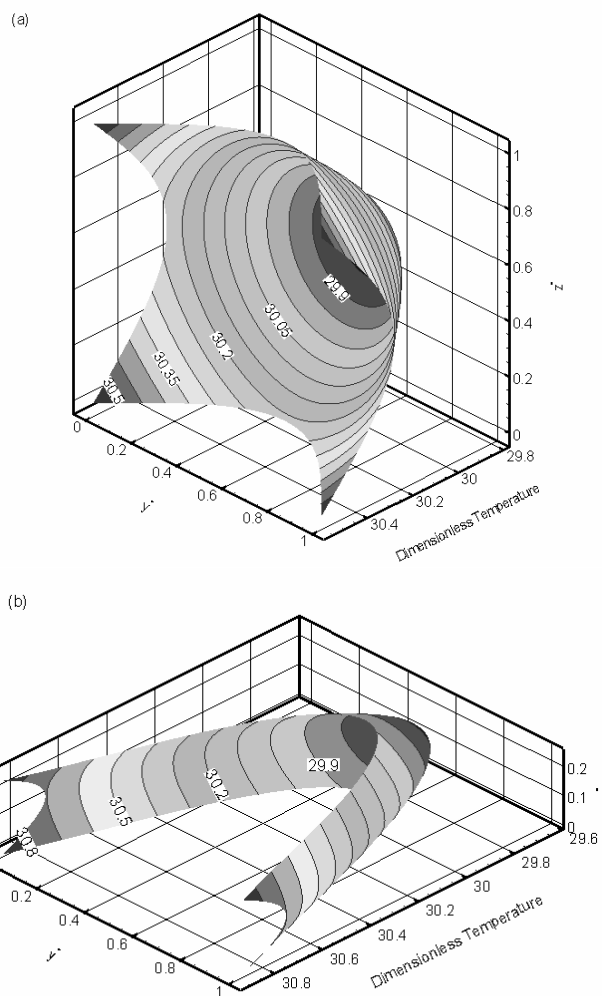


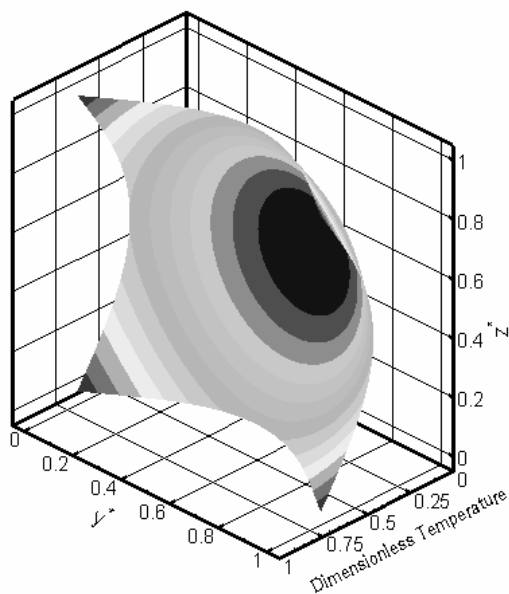
Fig. 2. Temperature contours of nonslip flow with constant wall heat flux at $x^+=15$ for (a) $\gamma=1$ and (b) $\gamma=0.25$

is a measure of temperature jump at the walls. It has no influence on temperature distribution in the domain and also on Nusselt number in nonslip flow, but it affects the magnitude of Nusselt number when $\beta' \neq 0$.

Fig. 5 reveals that for $\beta = 0.1$ Nusselt number augments with increasing β' whereas for $\beta = 1.667$ the trend is reversed. This can be explained in such a way that increase in momentum exchange is dominant over increase in temperature jump due to small β in the case $\beta=0.1$; however when β is large, the temperature jump prevails, so Nusslet number diminishes.

From the discussion above, one may result that there is a marginal value for β called β_m here. Beyond this value, Nusslet number always decreases as β' increases. Fig. 6 reveals the same trend as the former case for variation of Nu except in the range $m < -8$ for $\beta = 0.1$. As explained earlier $\beta = 0.1$ can be a marginal β for $m \approx -8$ and $\gamma = 0.5$, so trend of

(a)



(b)

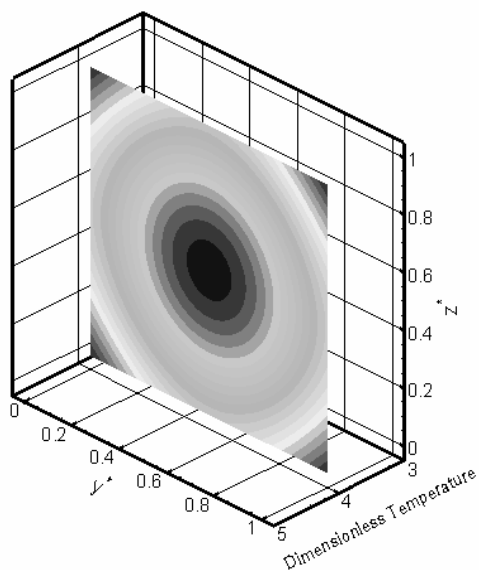


Fig. 3. Temperature contours of nonslip flow for $m = -1$ and $\gamma = 1$ at (a) $x^+ = 0.1$ and (b) $x^+ = 15$

Nu almost reverses at this point that means the temperature jump overrides the effect of velocity slip at the walls.

Fig. 7 gives the similar results for $\gamma = 0.25$, but in this case, m is varied from -1 to 10. As Shah and London [13] have shown for a circular tube, there is a certain range for m in where the results for Nusslet number are valid. Here is the same for rectangular microchannel. Consequently the range of allowed values for m restricts the results.

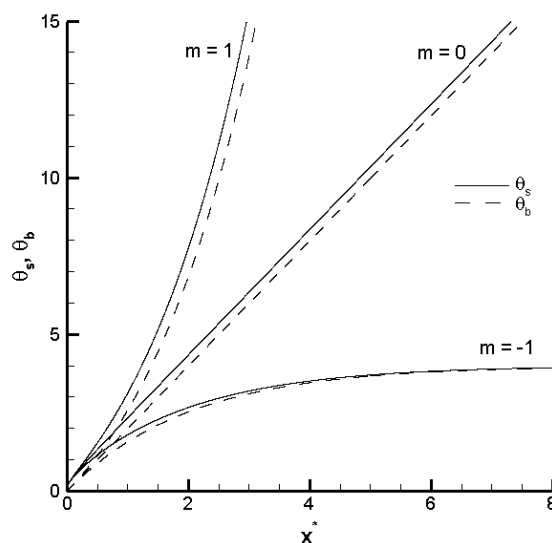


Fig. 4. Variations of θ_s and θ_b with longitudinal coordinate for three different values of m , $\gamma = 1$ and $\beta' = 0$

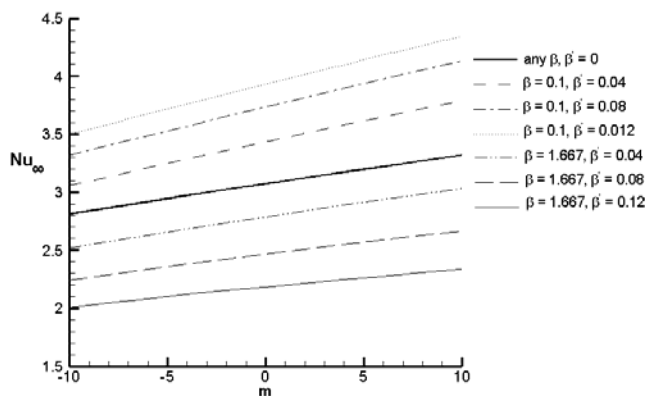


Fig. 5. Fully-developed Nusselt number for $\gamma = 1$ as a function of β' , β and m

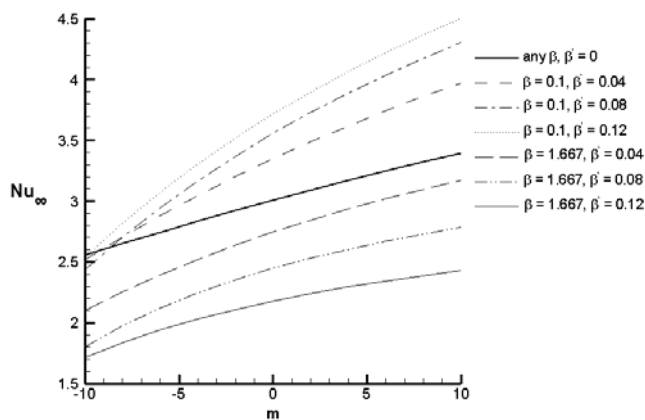


Fig. 6. Fully-developed Nusselt number for $\gamma = 0.5$ as a function of β' , β and m

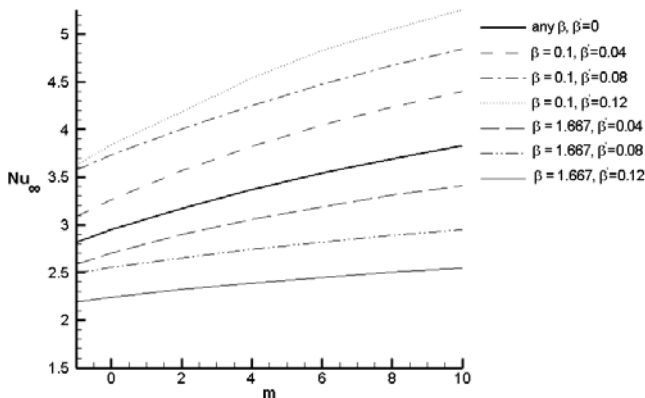


Fig. 7. Fully-developed Nusselt number for $\gamma=0.25$ as a function of β' , β and m

IV. CONCLUSION

The slip flow convection heat transfer in a rectangular microchannel with exponential wall heat flux has been studied numerically using finite-difference method. The rarefaction effects introduced to the problem include slip velocity and temperature jump. β and β' are considered as measures of these effects. It is found that Nusselt number does not change severely with aspect ratio when the peripherally-constant temperature hypothesis is not held. Furthermore, the variation of Nu against rarefaction parameters depends on the value of β . For large β , Nusselt number decreases as the velocity slip augments. In contrast for small β , Nusselt number increases as the velocity slip increases and dominates the temperature jump. This is true for all values of parameter m and there is a specific marginal β for each m .

V. REFERENCES

[1] A. Beskok, G.E. Karniadakis, Simulation of heat and momentum transfer in complex micro geometries, *J. Ther. Heat Transfer* 8 (4) (1994) 647-653.
 [2] E.B. Arkilic, K.S. Breuer, M.A. Schmidt, Gaseous flow in microchannels, in: *Application of microfabrication to Fluid Mechanics*, ASME FED, 197, 1994, pp. 57-66.
 [3] E.G.R. Eckert, R.M. Drake, Jr., *Analysis of Heat and Mass Transfer*, McGraw-Hill, New York, 1972, pp. 467-486.
 [4] E.M. Sparrow, S.H. Lin, Laminar heat transfer in tubes under slip-flow conditions, *ASME J. Heat Transfer* 84 (4) (1962) 363-639.
 [5] F.E. Larrode, C. Housiadas, Y. Drossinos, Slip-flow heat transfer in circular tubes, *Int. J. Heat Mass Transfer* 43 (2000) 2669-2680.
 [6] G. Tunc, Y. Bayazitoglu, Heat transfer in rectangular microchannels, *Int. J. Heat Mass Transfer* 45 (2002) 765-773.

[7] H.P. Kavehpour, M. Faghri, Y. Asako, Effects of compressibility and rarefaction on gaseous flows in microchannels, *Numer. Heat Transfer Part A* 32 (1997) 677-696.
 [8] J.C. Shih, C. Ho, J. Liu, Y. Tai, Monatomic and polyatomic gas flow through uniform microchannels, in: *1996 National Heat Transfer Conference, Micro Electro Mechanical Systems (MEMS)*, Atlanta, GA, DSC 59 (1996) 197-203.
 [9] N.G. Hadjiconstantinou, O. Simek, Constant-wall-temperature Nusselt number in micro and nano-channels, *J. Heat Transfer* 124 (2002) 356-364.
 [10] R. Goniak, G. Duffa, Corrective term in wall slip equations for Knudsen layer, *J. Thermophys.* 9 (1995) 383-384.
 [11] R.F. Barron, X.M. Wang, R.O. Warrington, T.A. Ameel, Evaluation of the eigenvalues for the Graetz problem in slip flow, *Int. J. Heat Mass Transfer* 23 (4) (1996) 563-574.
 [12] R.F. Barron, X.M. Wang, T.A. Ameel, The Graetz problem extended to slip flow, *Int. J. Heat Transfer* 40 (8) (1997) 1817-1823.
 [13] R. K. Shah, A. L. London, *Laminar Flow Forced Convection in Ducts*, Advances in Heat Transfer, Academic Press, New York, 1978.
 [14] R.M. Inman, Heat transfer for laminar slip flow of a rarefied gas in a parallel plate channel or a circular tube with uniform wall temperature, NASA TN, 1964, D-2213.
 [15] S.P. Yu, T.A. Ameel, Slip-flow convection in isoflux rectangular microchannel, *ASME J. Heat Transfer* 124 (2002) 346-355.
 [16] S.P. Yu, T.A. Ameel, Slip-flow low Peclet number thermal entry problem within a flat microchannel subject to constant wall temperature, in: *Proc. Heat Transfer and Transport Phenomena in Microsystems*, Banff, Alberta, Canada, 2000.
 [17] T.A. Ameel, R.F. Barron, X.M. Wang, R.O. Warrington, Laminar forced convection in a circular tube with constant heat flux and slip flow, *Microscale Thermophys. Eng.* 1 (4) (1997) 303-320.
 [18] W.M. Rohsenow, J.P. Hartnett, E.N. Ganic, *Handbook of Heat Transfer Applications*, McGraw-Hill, New York, 1985.
 [19] Y. Asako, Heat Transfer characteristics of gaseous flow in a micro-tube, in: *Second International Conference on Microchannels and Minichannels*, June 17-19, Rochester, New York, USA, 2004, pp. 305-311.